# Evaluation of Effective Parameters on EGR/Blowby Distribution

**P. Bashi Shahabi[1], H. Niazmand and M. R. Modarres Razavi**

[1] pbshahabi@yahoo.com

**Abstract**

Increase of environmental pollution and restricted emission legislations have forced companies to produce automobiles with lower air pollutants. In this respect, discharge of blowby gases into the environment has been prohibited and their recirculation into the combustion chamber is proposed as an alternative solution. In addition, using EGR technique to control and reduce nitrogen oxides in internal combustion engines has been quite effective. An important common feature of these two methods is the fact that improper EGR/blowby distribution leads to the increase in other pollutants and the significant engine power reduction. Therefore, the study of important factors in maldistribution of the injected gases is of great practical importance. Besides the injection position that has significant role on distribution of injected gases, it seems that other parameters such as engine speed, injection velocity and angle may affect the distribution of injected gases. In this numerical study, a new technique is used to determine the effect of these parameters on distribution of injected EGR or blowby gases into the EF7 intake manifold. Numerical calculations are performed for three injection velocities, five injection angles and three different engine speeds. It was found that recirculated gases distribution is slightly influenced by the injection angle and injection velocity, while the engine speed is the most influential factor.

***Keywords***: *Recirculated gases, Blowby gases, Injection angle, Injection velocity, Engine speed, Maldistribution*

## 1. INTRODUCTION

Air pollution in the present world if not considered as the most important issue of human society, it definitely contributes to the major problems of the world. Due to the increasing pressure on car makers to observe the new emissions standards, designers use any means that even has a little impact on reducing engine emissions. From years ago, EGR (Exhaust Gas Recirculation) technique has been effectively used to control and reduce nitrogen oxides (NOx) produced by internal combustion engines [1-6]. In this method, a percentage of the combustion products recirculated from exhaust system to the intake manifold. By reducing the amount of burned fuel, the combustion temperature would decrease. Since temperature is the most important factor in the nitrogen oxides production, this method would help to control NOx emission in vehicle engines. On the other hand, the existing emission regulations do not allow engine manufacturers to discharge blowby gases into the environment. The employed approach is recirculating blowby gases into the combustion chamber and burning them [7]. An interesting point is that both methods work based on recirculating gases into the intake manifold. If the gas recirculation system is not carefully employed, significant reduction on engine power and increase of other pollutants may be resulted. One of the consequences of using an inappropriate recirculation system is referred to as maldistribution of injected EGR/blowby gases [8-12], which is basically a measure of the non- uniformity in distribution of injected gases. Therefore using a system, which distributes the recirculated gases uniformly between the intake runners, seems to be inevitable. In the previous studies [13-15], it was indicated that the position and number of EGR/blowby injection points have an important influence on distribution of injected gases between cylinders.

So far, applied techniques to study the distribution of recirculated EGR/blowby gases are limited to the $CO_2$ injection and thermal methods. Recently the authors introduced a new method based on particle tracking to study the distribution of the recirculated gases and described the advantages of this technique in respect to the other methods [13 and 14].

Previous studies have mostly been focused on locating the position of injected EGR/blowby gases, which resulted less maldistribution between cylinders.

However, the effects of other factors, such as injection velocity, injection angle and engine speed that seem to be effective on this distribution, have not been investigated. Due to benefits of the particle tracking method, the effects of these factors on distribution of EGR/blowby gases can be examined properly. In the present study, the effects of the above parameters on distribution of recirculated EGR/blowby gases in the EF7 intake manifold are analyzed.

## 2. EXAMINATION OF RECIRCULATED EGR/BLOWBY GASES DISTRIBUTION METHODS

To study the maldistribution of recirculated gases thermal and gas injection methods in addition to the new particle tracking technique can be employed. The two previous methods have been used in the both numerical and experimental investigations. Torres and Henriot [8] in a numerical study and Siewert et al. [9] in a combined experimental and numerical examination studied EGR distribution in an intake system by using a non-air gas injection into the manifold. In addition, in an experimental study Green [11] proposed a new method for determining maldistribution of recirculated EGR gases by injecting $CO_2$ into the intake manifold. Besides, by employing thermal method in a practical study William et al. [10] examined the effects of geometrical parameters on EGR/air mixture in the intake manifold.

To clarify the advantages and disadvantages of these methods, a brief description of them are presented as follow.

### 2. 1. Gas Injection Method

Distribution of EGR/blowby recirculated gases in a manifold can be studied by considering two different types of gases. In this method, intake air is the main flow and the second gas, which is typically $CO_2$ or HC, plays the role of recirculated EGR/blowby gases. $CO_2$ or HC, with a specified mass flow rate are injected into the intake manifold from certain location(s). By measuring or calculating the mass fraction of the second species ($CO_2$, or HC) at the end of each runner, the percentage of injected gases entered into each cylinder can be estimated.

Although this method is relatively accurate, expensive instruments are required for experimental studies and it is time consuming when numerically simulated, such that one time step of a flow field calculation including 700,000 cells takes about 5 to 6 minutes on a 2.4 GHz (Intel E6400) Core 2 Duo processor with 2 GB of DDR2 Ram. Since each time step equals 2 degree of crankshaft rotation and each cycle including 360 time steps computations, only one cycle takes nearly 30 to 36 hours. In addition, if steady state conditions have to be achieved at least 8 to 10 cycles must be solved. On the other hand, the case of simultaneous injections from two or multiple points takes enormous time which is not practical with this method.

### 2. 2. Thermal Method

In thermal method, recirculated EGR/blowby gas is replaced by a hot gas injection. Due to the temperature difference between the injected gas and incoming air, the temperature of the mixture is different from the initial temperature of air and injected gases. Obviously, the mixture temperature indicates the amount of injected gases mixed with air. Considering a given flow rate of air and injected gases, contribution of each cylinder from injected gases can be estimated by measuring or calculating the flow temperature at the end of each intake runner. Reference [10] assumed negligible heat transfer from intake manifold and used energy balance to obtain the following equation for mass flow rate of injected gases at each runner.

$$\frac{\dot{m}_{EGR/Blowby,i}}{\dot{m}_{EGR/Blowby}} = \frac{\dot{m}_{air} + \dot{m}_{EGR/Blowby}}{N\,\dot{m}_{EGR/Blowby}} \times \frac{T_i - T_{air}}{T_{EGR/Blowby} - T_{air}} \qquad (1)$$

In the above equation $\dot{m}_{EGR/Blowby,i}$, $\dot{m}_{air}$, and $\dot{m}_{EGR/Blowby}$ represent EGR/blowby mass flow rate which is received by the i$^{th}$ runner, total air mass flow rate of intake manifold and total recirculated EGR/blowby mass flow rate, respectively. In addition, N determines the number of cylinders or runners of intake manifold. Besides, $T_{air}$ stands for incoming air temperature, $T_{EGR/Blowby}$ indicates the temperature of recirculated EGR/blowby gases, and $T_i$ is the temperature of the mixture, which is passing through each runner.

In an experimental study, a thermometer sensor should be installed on each runner of the intake manifold. Installation location and distance from inner wall of the runner have an important impact on the results accuracy [10].

Numerical simulation on a system with similar configuration mentioned earlier, approximately takes 3.5 minutes for each time step. Compared with $CO_2$ injection method, convergence time is reduced because there is no need to solve transport equations. However, like $CO_2$ injection, this method requires spending a lot of time to perform a comprehensive study on the distribution of recirculated EGR/blowby gases. Moreover, it should be noted that since thermal method is based on temperature difference between injected gas and incoming air flow, this method is more suitable for hot EGR.

### 2. 3. Particle Tracking Method

In this method instead of injecting gas from desired position(s), massless particles are injected into the flow field. Particles under the influence of incoming air distribute in the flow field and can be tracked independently. Therefore, it is possible to study simultaneous injections from different locations with various conditions (e.g. different velocities or injection angles). This means that the method is able to identify the maldistribution of recirculated EGR/blowby gases for several injection locations and conditions, with just one flow simulation. Since in this method particles are encoded the injection location and condition of each trapped particle can be determined easily. The method can also be used to investigate the degree of maldistribution for simultaneous EGR/blowby injection from two or more injection locations. In this research the Lagrangian discrete phase model of FLUENT which follows the Euler-Lagrange approach is employed to simulate the distribution of injected particles. In this approach, the fluid phase is treated as a continuum by solving the time-averaged Navier-Stokes equations, while the dispersed phase is solved by tracking a large number of particles. The dispersed phase can exchange momentum with the fluid phase. The trajectory of an injected particle is predicted according to the Newton's law of motion in a Lagrangian reference frame, where the resulting forces exerted on the particle are balanced with the particle inertia. All particles passing through each runner exit are considered as the contribution of the injected gas for that runner.

It must be emphasized that, when the mass flow rate of the recirculated EGR/blowby gases is large enough to affect the main airflow pattern in the plenum the mass flow rate of the injected gases should be taken into account. It is obvious that in such conditions the study of simultaneous multi-injection locations for different conditions with just one simulation is not possible and similar to pervious methods each case should be solved separately. Based on different numerical experimentations it was found that as long as the mass flow rates of the recirculated gases are less than 5% of the main airflow, the effect of the injected gas mass flow rate could be safely ignored. More details in this regard can be found in [14].

Required time for simulation with particle tracking method is approximately the same as thermal method. Increasing the injection locations and conditions leads to slight increase in simulation time, which is quite reasonable.

In the present study, the effects of injection velocity, angle and engine speed on distribution of recirculated EGR/blowby gases are investigated. Due to the multiplicity of situations and conditions particle tracking is the most suitable method for the present study.

## 3. EFFECTIVE PARAMETERS ON RECIRCULATED EGR/BLOWBY DISTRIBUTION

It seems that many parameters such as injection location, injection velocity, injection angle and engine speed affect the distribution of recirculated EGR/blowby in an intake manifold. Except for the injection location, which is found from previous studies [13, 14] that has a considerable influence on the distribution of the recirculated gases, the effect of other parameters on distribution of injected gases have not been studied so far. Therefore, the purpose of this study is to examine the effects of these factors on distribution of injected gases for intake manifold of the EF7 engine.

## 4. GEOMETRICAL MODEL

It is common to consider the plenum as a proper place for EGR/blowby injection points due to the presence of a satisfactory and stable suction pressure and ease of access. The intake manifold of the EF7 engine consisting of a plenum and four runners is shown in Fig. 1.

In order to investigate the effect of above mentioned parameters on EGR/blowby recirculation,

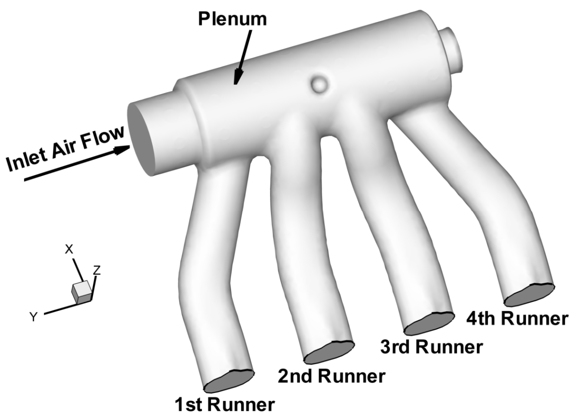


**Fig. 1.** Intake manifold configuration of the EF7 engine

thirty-nine injection locations are considered on the plenum to cover almost all possible injection cases. As shown in Fig. 2 injection points are placed regularly on 8 axial lines with angular step of 45 degree in azimuthal direction. Depending on the angular location, each axial line includes 1 to 7 injection points along the plenum. The above classification provides the opportunity to categorize the distributive behavior of each group of injection location on the intake plenum.

## 5. GOVERNING EQUATIONS

It is assumed that a compressible and turbulent flow is established during an engine working cycle. The governing equations for a transient compressible flow are the continuity, momentum, and energy equations along with the equation of state are expressed as:

$$\frac{\partial \rho}{\partial t} + \nabla \cdot \left(\rho \vec{V}\right) = 0 \tag{2}$$

$$\rho\left(\frac{\partial \vec{V}}{\partial t}\right) + \left(\vec{V} \cdot \nabla\right)\vec{V} = -\nabla p + \nabla \cdot \vec{\tau} \tag{3}$$

$$\rho C_p \left(\frac{\partial T}{\partial t}\right) + \left(\vec{V} \cdot \nabla\right) T = -\nabla \cdot \left(k \nabla T\right) \tag{4}$$

$$p = \rho R T \tag{5}$$

where $\rho$ is density, $\vec{V}$ is the velocity vector, $p$ is pressure, $T$ is temperature, and $\vec{\tau}$ is stress tensor which is defined as:

$$\vec{\tau} = \mu \dot{\vec{\gamma}} = \mu \left[ \nabla \vec{V} + \left(\nabla \vec{V}\right)^{tr} \right] \tag{6}$$

Based on the previous studies [15-17], k-ε turbulence modeling adequately represents the turbulence characteristics of the present flow. In the k-å model the turbulent kinetic energy, k, and the dissipation rate, $\varepsilon$, can be obtained from the following equations:

$$\rho\left(\frac{\partial k}{\partial t}\right) + \left(\vec{V} \cdot \nabla\right) k = \nabla \cdot \left(\left[\mu + \frac{\mu_t}{\sigma_k}\right] \nabla k\right) + G_k - \rho\varepsilon \tag{7}$$

$$\rho\left(\frac{\partial \varepsilon}{\partial t}\right) + \left(\vec{V} \cdot \nabla\right) \varepsilon = \nabla \cdot \left(\left[\mu + \frac{\mu_t}{\sigma_\varepsilon}\right] \nabla \varepsilon\right) + C_{1\varepsilon} \frac{\varepsilon}{k} G_k - C_{2\varepsilon} \rho \frac{\varepsilon^2}{k} \tag{8}$$

where k is turbulent kinetic energy and $\varepsilon$ is the

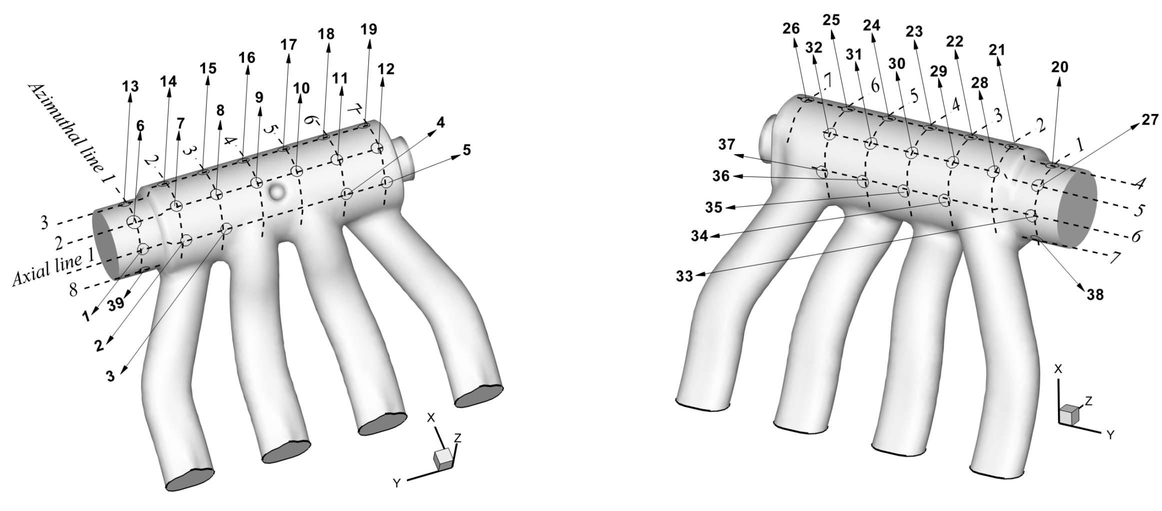


**Fig. 2.** Considered injection points (39 cases) for EGR/blowby recirculation on the manifold plenum

dissipation rate. $G_k$ represents the generation of turbulence kinetic energy due to the mean velocity gradients, calculated by $G_k = -\rho \overline{u_i' u_j'} \frac{\partial u_j}{\partial x_i}$. The turbulent viscosity defined as $\mu_t = \rho C_\mu \frac{\varepsilon^2}{k}$, while $\sigma_k$ and $\sigma_\varepsilon$ are the turbulent Prandtl numbers for $k$ and $\varepsilon$ equations, respectively. In the above $C_{1\varepsilon}$, $C_{2\varepsilon}$, $C_\mu$, $\sigma_k$ and $\sigma_\varepsilon$ are all taken to be constant and given respectively the values 1.44, 1.92, 0.09, 1.0, and 1.3.

### 5.1. Numerical Method and Boundary Conditions

The Fluent 6.3 software, which is based on a control volume technique, is employed for solving the governing equations. In addition, the Gambit software is utilized for mesh generation and performing geometrical modifications.

Since the flow field is time dependent, the governing equations are solved over a full engine working cycle. Therefore, the required time dependent boundary conditions are obtained from a 1-D simulation by GT-Power software, which is fully calibrated for the EF7 engine. The uniform (averaged) fluid pressure at four runner outlets and air mass flow rate on the plenum inlet are obtained on the basis of piston crank angle and time. These four averaged pressures, which are also adjusted for full load and part loads at different engine speeds are specified as the runner outlets boundary conditions for the 3-D calculations. As for the inlet boundary condition, the mass flow rate is specified. The boundary conditions in 3-D simulations for the open runners are basically corresponding to the mass driven condition for internal flows. However, for the runners in closed condition no slip boundary conditions are applied, while adiabatic walls are considered. The adopted boundary conditions can properly resolve the pressure waves generated right at the closing and opening time of the runners.

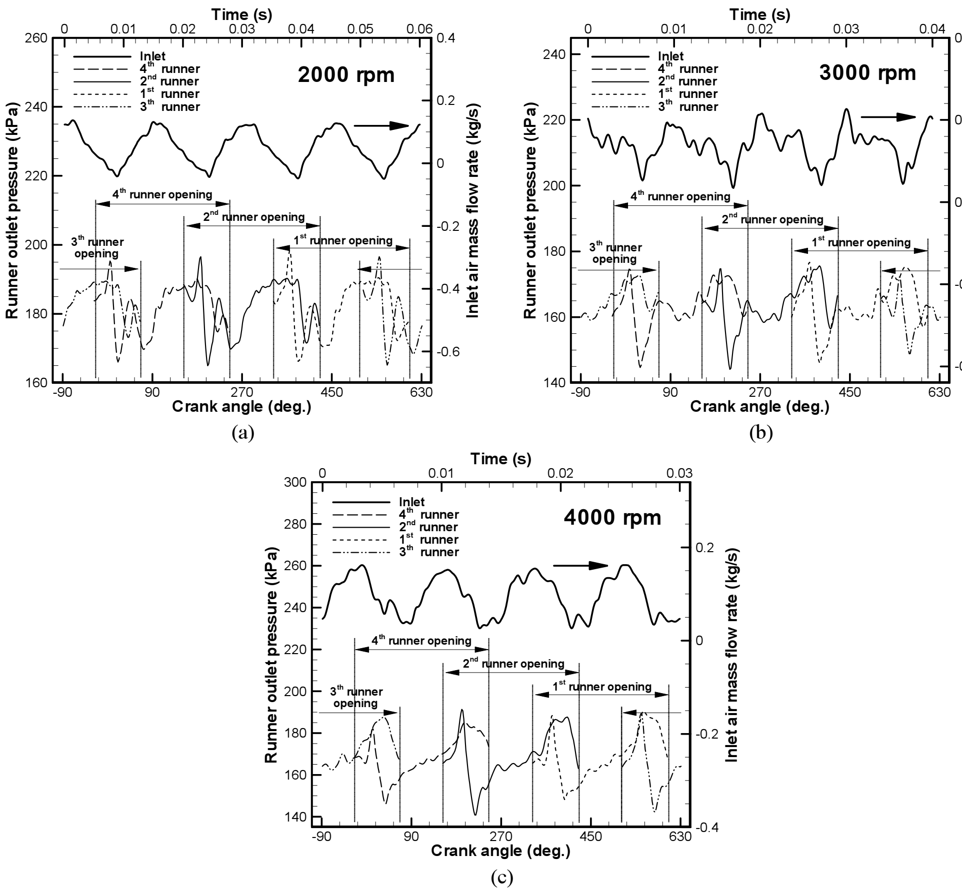


**Fig. 3.** Time variations of mass flow rate at the plenum inlet and pressure at the four runner outlets for one engine cycle at full load and (a) 2000, (b) 3000, and (c) 4000 rpm engine speed from 1-D numerical simulation

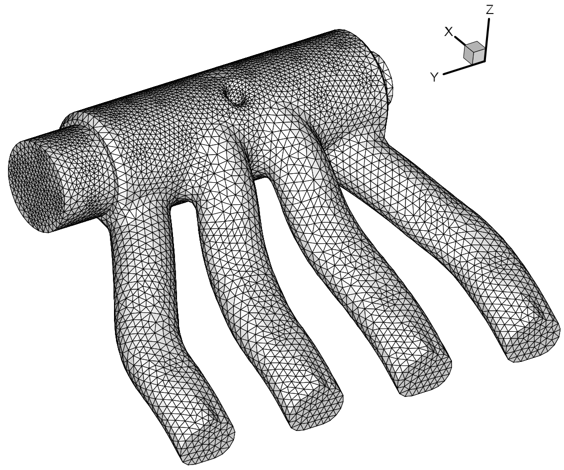


**Fig. 4.** Intake manifold mesh distribution with 73140 tetrahedral cells

The time variations of the plenum inlet mass flow rate and the runners outlet pressure at full load and 2000, 3000, and 4000 rpm engine speed conditions according to the 1-D simulation model are presented in Fig. 3. The piston crank angle is shown on the lower horizontal axis, while the upper horizontal axis indicates the corresponding time in one engine working cycle. In addition, the right vertical axis represents the intake mass flow rate, while the left vertical axis shows the static pressure at the outlet of each runner. It should be noted that the EF7 as a four cylinder engine has standard firing order (1-3-4-2), which can be identified in the order of runners opening as shown in Fig. 3.

## 6. MESH INDEPENDENCY

Unstructured mesh with tetrahedral cells generated by Gambit 3.2.16 software is found to be suitable for the complex configuration of flow geometry. All computations in this research are performed on a mesh system of 73140 cells as shown in Fig. 4. Different mesh distributions are examined for the grid independency tests with the finest mesh system of 180496 cells. The results indicate that the maximum mass flow rate difference between the adopted and the finest mesh systems is less than 5%.

It is worth mentioning that the CPU time of the finest mesh system is about two times longer than that of the adopted mesh system.

## 7. Numerical Model Validation

1-D simulation by GT-Power software, fully calibrated with the experimental data, is widely used for the pre-design of intake/exhaust system components and engine performance analysis. Since the 1-D model is calibrated with the experimental data of the EF7 engine, the numerical validation can be performed by comparing the 1-D and 3-D numerical results. Considering the significant effects of intake air flow on the distribution of recirculated gases in the intake manifold, the air mass flow rate in plenum and runners are compared in Fig. 5. This figure shows the time variations of the air mass flow rates of each

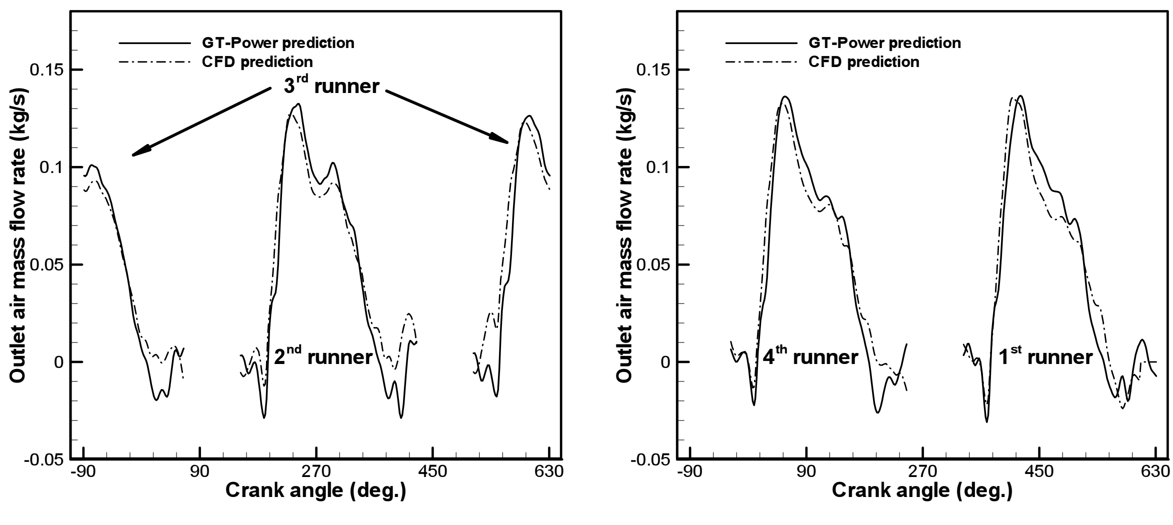


**Fig. 5.** Time variations of air outlet mass flow rate for each runner for 3-D and 1-D numerical simulations

**Table 1.** Four injection locations with the least and the most maldistributions for the base case injection velocity of 3.4 m/s

| Injection location | Contribution of each runner from the total injected EGR/blowby gases (%)/Base condition | | | | **maldistribution** |
|---|---|---|---|---|---|
| | 1st runner | 2nd runner | 3rd runner | 4th runner | |
| 34 | 13.32 | 27.34 | 33.68 | 25.65 | **5.84** |
| 23 | 10.02 | 37.76 | 28.03 | 24.18 | **7.90** |
| 24 | 10.89 | 37.65 | 23.23 | 28.23 | **7.94** |
| 7 | 27.17 | 41.78 | 22.40 | 8.65 | **9.47** |
| 20 | 0.34 | 1.58 | 23.62 | 74.46 | **24.73** |
| 36 | 0.03 | 0.06 | 25.36 | 74.56 | **24.96** |
| 37 | 0.00 | 0.00 | 18.97 | 81.03 | **28.02** |
| 5 | 0.52 | 0.87 | 5.73 | 92.88 | **33.94** |

**Table 2.** Four injection locations with the least and the most maldistributions for the injection velocity of 5.1 m/s

| Injection location | Contribution of each runner from the total injected EGR/blowby gases (%) | | | | **maldistribution** |
|---|---|---|---|---|---|
| | 1st runner | 2nd runner | 3rd runner | 4th runner | |
| 34 | 13.31 | 27.37 | 33.35 | 25.98 | **5.85** |
| 23 | 11.15 | 36.86 | 27.98 | 24.01 | **7.42** |
| 24 | 11.36 | 38.74 | 23.29 | 26.61 | **7.68** |
| 7 | 26.69 | 42.56 | 25.22 | 8.51 | **9.62** |
| 20 | 0.35 | 1.65 | 23.74 | 74.26 | **24.63** |
| 36 | 0.04 | 0.03 | 25.13 | 74.80 | **24.97** |
| 37 | 0.00 | 0.00 | 19.05 | 80.95 | **27.97** |
| 5 | 0.25 | 0.83 | 5.64 | 93.27 | **34.14** |

**Table 3.** Four injection locations with the least and the most maldistributions for the injection velocity of 10.2 m/s

| Injection location | Contribution of each runner from the total injected EGR/blowby gases (%) | | | | **maldistribution** |
|---|---|---|---|---|---|
| | 1st runner | 2nd runner | 3rd runner | 4th runner | |
| 34 | 13.28 | 27.26 | 33.62 | 25.83 | **5.56** |
| 23 | 11.44 | 36.82 | 28.72 | 23.02 | **7.77** |
| 24 | 11.45 | 38.01 | 23.87 | 26.67 | **7.34** |
| 7 | 26.65 | 42.49 | 22.48 | 8.38 | **9.57** |
| 20 | 0.25 | 1.56 | 23.97 | 74.23 | **24.61** |
| 36 | 0.03 | 0.04 | 25.19 | 74.74 | **24.97** |
| 37 | 0.00 | 0.00 | 19.02 | 80.97 | **27.99** |
| 5 | 0.33 | 1.38 | 5.24 | 93.06 | **34.03** |

runner for 3-D simulation and 1-D model for 3000 rpm engine speed, where similar trend can be observed. It is interesting to note that in all cases the maximum discrepancies occur near the valve opening and closing. Furthermore, the maximum difference between the integrated mass flow rate of each runner with its corresponding value in 1-D model is less than 8%. Similar results are obtained for engine speeds of 2000 and 4000 rpm.

## 8. STUDY OF EFFECTIVE PARAMETERS ON RECIRCULATED EGR/BLOWBY DISTRIBUTION

The effects of injection velocity, injection angle and engine speed on the distribution of recirculated EGR/blowby are studied in the following sections. In the present study, the base EGR/blowby injection conditions are defined as injection velocity of 3.4 m/s, injection angle of 90 degrees with respect to the

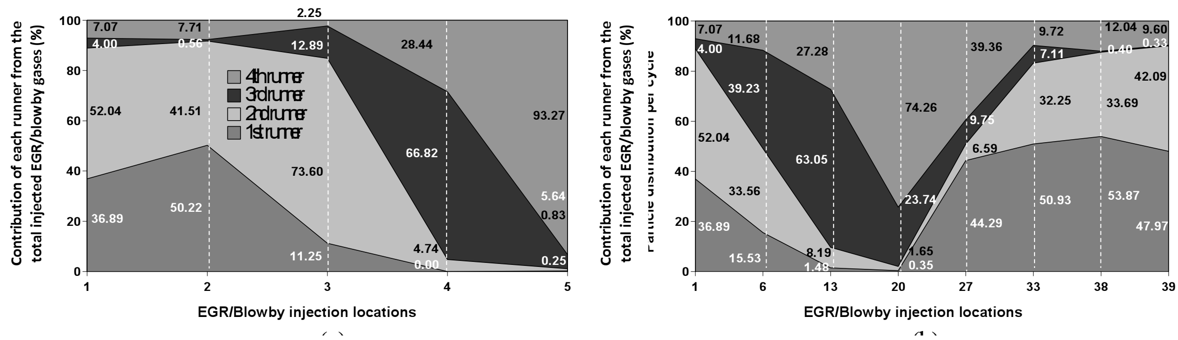


**Fig. 6.** Contribution of each runner from the total injected EGR/blowby gases for the injection velocity of 5.1 m/s and injection points located: (a) on the first axial line (b) on the first azimuthal line

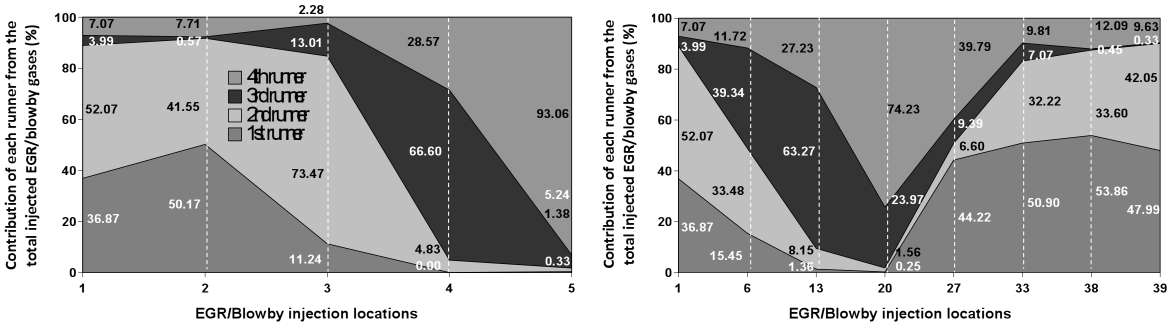


(a) (b)

**Fig. 7.** Contribution of each runner from the total injected EGR/blowby gases for the injection velocity of 10.2 m/s and injection points located: (a) on the first axial line (b) on the first azimuthal line

injection surface and engine speed of 3000 rpm. As a criterion for evaluating the maldistribution of the injected gases, the normalized distributions of the injected gases for each runner are compared with the ideal distribution, which is basically 25%. The average of these differences for the four runners indicates the maldistribution of the corresponding injection situation. As mentioned earlier, particle tracking method can be confidently applied when the injected mass flow rate is relatively small as compare to the main air flow in the plenum. Therefore, in the present study the mass flow rate of the injected gases is taken as 1% of the air mass flow rate.

## 8. 1. Injection Velocity Effect

To study the effect of injection velocity on EGR/blowby distribution between cylinders, two different injection velocities in addition to the base case injection velocity (3.4 m/s) are considered. These injection velocities are 5.1 m/s and 10.2 m/s, which are basically 1.5 and 3 times larger than the base case injection velocity. For a given mass flow rate of EGR/blowby the increase in injection velocity requires reduction in injection cross sectional area, which has its own numerical limitations. Therefore, injection velocities higher than 3 times the base injection velocity are not considered here. The contribution of each runner from the total injected EGR/blowby gases are presented in tables 1-3 for injection velocities of 3.4, 5.1, and 10.2 m/s, respectively. It should be noted that these values represent the percentage of EGR/blowby gases received by each cylinder during the working cycle. In table 1 four injection locations corresponding to the least and the most maldistributions are listed for the base injection velocity. For comparison, the same injection locations as those in table 1are listed for the injection velocities of 5.1 and 10.2 m/s in tables 2 and 3, respectively. Results indicate that in general the EGR/blowby gases distribution is slightly influenced

**Table 4.** Results of injection angle for 1-injection point compared with the base condition results.

| 1-Injection point | Contribution of each runner from the total injected EGR/blowby gases (%) | | | | **maldistribution** |
|---|---|---|---|---|---|
| | 1st runner | 2nd runner | 3rd runner | 4th runner | |
| Base condition | 37.20 | 51.77 | 4.00 | 7.03 | **19.49** |
| Inj. Angle-1 | 37.07 | 51.13 | 4.07 | 7.10 | **19.42** |
| Inj. Angle-2 | 37.45 | 51.54 | 3.92 | 7.09 | **19.50** |
| Inj. Angle-3 | 37.71 | 51.12 | 3.99 | 7.18 | **19.42** |
| Inj. Angle-4 | 37.56 | 51.36 | 3.93 | 7.15 | **19.46** |

**Table 5.** Eight injection locations with the least maldistribution for 2000 rpm engine speed.

| Injection location | Contribution of each runner from the total injected EGR/blowby gases (%) | | | | **maldistribution** |
|---|---|---|---|---|---|
| | 1st runner | 2nd runner | 3rd runner | 4th runner | |
| 6 | 20.22 | 33.95 | 31.67 | 14.16 | **7.81** |
| 7 | 19.66 | 30.76 | 38.25 | 11.33 | **9.50** |
| 34 | 25.87 | 34.85 | 37.06 | 2.22 | **11.39** |
| 38 | 48.02 | 22.25 | 16.09 | 13.63 | **11.51** |
| 8 | 22.62 | 49.53 | 14.43 | 13.42 | **12.26** |
| 39 | 49.61 | 25.06 | 11.85 | 13.49 | **12.33** |
| 1 | 40.09 | 36.44 | 12.43 | 11.04 | **13.26** |
| 15 | 2.27 | 20.45 | 50.00 | 27.27 | **13.64** |

**Table 6.** Eight injection locations with the least maldistribution for 3000 rpm engine speed.

| Injection location | Contribution of each runner from the total injected EGR/blowby gases (%)/Base condition | | | | **maldistribution** |
|---|---|---|---|---|---|
| | 1st runner | 2nd runner | 3rd runner | 4th runner | |
| 34 | 13.32 | 27.34 | 33.68 | 25.68 | **5.84** |
| 23 | 10.02 | 37.76 | 28.03 | 24.18 | **7.90** |
| 24 | 10.89 | 37.65 | 23.23 | 28.23 | **7.94** |
| 7 | 27.17 | 41.78 | 22.40 | 8.65 | **9.47** |
| 16 | 14.21 | 42.14 | 27.61 | 16.04 | **9.88** |
| 6 | 15.18 | 33.66 | 39.18 | 11.97 | **11.42** |
| 15 | 20.29 | 47.16 | 26.81 | 5.74 | **11.99** |
| 22 | 5.42 | 20.09 | 32.75 | 41.74 | **112.25** |

**Table 7.** Eight injection locations with the least maldistribution for 4000 rpm engine speed.

| Injection location | Contribution of each runner from the total injected EGR/blowby gases (%) | | | | **maldistribution** |
|---|---|---|---|---|---|
| | 1st runner | 2nd runner | 3rd runner | 4th runner | |
| 15 | 16.56 | 23.24 | 42.15 | 17.96 | **8.58** |
| 7 | 38.76 | 28.63 | 27.00 | 5.61 | **9.69** |
| 28 | 37.06 | 16.00 | 12.05 | 34.89 | **10.97** |
| 6 | 23.60 | 33.91 | 38.48 | 4.02 | **11.19** |
| 27 | 36.48 | 13.93 | 12.99 | 36.60 | **11.54** |
| 8 | 33.80 | 40.34 | 11.43 | 14.43 | **12.07** |
| 16 | 7.88 | 17.33 | 27.31 | 47.49 | **12.40** |
| 34 | 15.60 | 32.28 | 45.30 | 6.82 | **13.76** |

by the injection velocities. In addition, Figs 6 and 7 display the EGR/blowby distribution of injection points, located on the first axial and azimuthal line, for injection velocities of 5.1 and 10.2 m/s, which also indicates that recirculated gases distributions between runners are not basically affected by the injection velocities.

### 8. 2. Injection Angle Effect

In the base injection conditions, particles are injected perpendicular to the both injection surface and the air flow stream in the plenum as shown in Fig. 8. To study the effects of injection angle of recirculated gases, four different angles in addition to the base one are considered for each injection location. These four angles, which are numbered from 1 to 4,

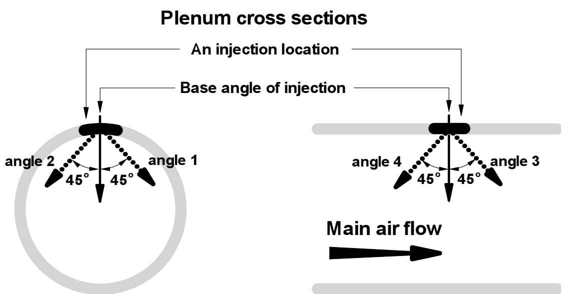


**Fig. 8.** Numbering scheme and orientation of different injection angles: (a) cross sectional plane (b)longitudinal plane

are well described in Fig. 8. Injection angles 1 and 2 are oriented with 45° from either side of the base injection direction in the cross sectional plane of the plenum (Fig. 8-a), while injection angles 3 and 4 (Fig. 8-b) are located in the longitudinal cross section of the plenum in the plane containing the base injection angle. Injection angle 3 is in the plenum main air flow direction, whereas injection angle 4 opposes the main flow direction. It is the advantage of the particle tracking method that can handle all five injection angles for all injection locations in just a single solution of the main air flow. Results for all injection locations indicate that distribution of the injected gases are almost independent of the orientation angle of the injected stream. As a sample, the contribution of each runners from the injected gases for different injection angles of injection location number one are listed in table 4. Clearly, the recirculated gases distributions are not affected by the injection angles, even for injection angles of 1 and 2. These two injection angles basically shoot the particles toward the plenum walls, where less mixing of the injected stream is expected with the main air flow.

### 8. 3. Engine Speed Effect

Among the different factors that are expected to affect the recirculated gases distributions, engine speed is the most influential parameters. Engine speed is directly related to the air mass flow rate through the plenum and the resulting velocity field, which then affects the recirculated gases distributions. Engine speeds of 2000 and 4000 rpm are examined beside the engine speed of 3000rpm considered as the base case condition. Since maldistribution ranks of injection points are greatly influenced by engine speed, for clarity, only eight injection points with the least maldistribution are considered here. In tables 5, 6, and 7 the contribution of each runner from the recirculating gases are listed for all three engine speeds of 2000, 3000, and 4000 rpm, respectively.

It can be seen that the four injection points of 6, 7, 15, and 34 are the only common injection points among all engine speeds with maldistribution ranging from about 5 to 13. In Fig. 2 the physical location of these injection points are shown. It is interesting to note that these injection points are located on each side of the plenum close to the inlet. Present data is of great importance in identifying the best injection point with the least maldistribution. Apparently, for the present case the best injection point would be either located between the axial lines of 2 and 3 or around the axial line of 6 in azimuthal direction. While in the axial direction, the injection point would not be located beyond the azimuthal line of 3 from the inlet.

## 9. CONCLUSIONS

In this numerical study, effects of injection velocity, injection angle, and engine speed on recirculated EGR/blowby distribution are investigated for the EF7 intake manifold and the following results are obtained:

a) Distributions of recirculated gases between cylinders are slightly influenced by the injection velocity and orientation. Since several injection velocities and injection angles for relatively large number of injection points distributed almost uniformly over the plenum have been examined in the present study, it can be concluded that this fact can be confidently applied to all intake manifold with almost similar design.

b) Distribution of recirculated gases are greatly influenced by the variations of engine speed. This is because the engine speed is directly related to the air mass flow rate, which affects the flow pattern through the plenum. Present results indicate that it might not be possible to locate a single injection point with least maldistribution for all engine speeds. As a result, the averaged performance of candidate injection points for all different engine speeds should be considered as the requirement for choosing the proper injection point.

c) The particle tracking method can serve as a proper tool for locating the most appropriate injection location of the recirculated gases. For the present case, it was found that injection locations on the plenum sides close to the inlet leads to the least maldistribution.

## 10. ACKNOWLEDGMENT

The authors would like to thank the Engine Research Center of Iran Khodro (IPCO), for supporting this research and helpful discussions.

## REFERENCES

[1] Ladomatos, N., Abdelhalim, S. M., and Zhao, H., “Effect of Exhaust Gas Recirculation Temperature on Diesel Engine Combustion and Emissions”, Journal of Automobile Engineering, 1998, Vol. 212.

[2] Alger, T., “Synergies between High EGR Operation and GDI Systems”, SAE paper 2008, No. 2008-01-0134.

[3] He, Y., Salemat, A., Reese, R., Vick, R., and Amer, A., “Effect of Intake Primary Runner Blockages on Combustion Characteristics and Emissions with Stoichiometric and EGR-Diluted Mixtures in SI Engines”, SAE paper 2007, No. 2007-01-3992.

[4] Millo, F., Pautasso, E., Pasero, P., Barbero, S., and Vennettilli, N., “An Experimental and Numerical Study of an Advanced EGR Control System for Automotive Diesel Engines”, SAE paper 2008, No. 2008-01-0208.

[5] Florea, R., Toraza, D., Henein, N., and Bryzk, W., “Transient Fluid Flow and Heat Transfer in the EGR Cooler”, SAE paper 2008, No. 2008-01-0956.

[6] Hountalas, D. T., Mavropoulos, G., and Zannis, T., “Comparative Evaluation of EGR, Intake Water Injection and Fuel-Water Emulsion as NOx Reduction Techniques for Heavy Duty diesel Engines”, SAE paper 2007, No. 2007-01-0120.

[7] Dhariwal, H. C., “Control of Blowby Emissions

and Lubricating Oil Consumption in I.C. Engines", Energy Convers. 1997, Vol. 38, No. 10-13, 1267-1274.

[8] Torres, A., Henriot, S., "Modeling the Effects of EGR Inhomogeneities Induced by Intake Systems in a Four-Valve Engine" SAE paper 1996, No. 961959.

[9] Siewert, R. M., Krieger, R. B., Huebler, M. S., Baruah, P. C., Khalighi, B., and Wesslau, M., "Modifying an Intake Manifold to Improve Cylinder-to-Cylinder EGR Distribution in a DI Diesel Engine Using Combined CFD and Engine Experiment", SAE paper 2001, No. 2001-01-3685.

[10] William, J., Dupont, A., Bazile, R., and Marchal, M., "Study of Geometrical Parameter Influence on Air/EGR Mixing", SAE paper 2003, No. 2003-01-1796.

[11] Green, R. M., "Measuring the Cylinder-to-Cylinder EGR Distribution in the Intake of a Diesel Engine during Transient Operation" SAE Paper 2000, No. 2000-01-2866.

[12] Partridge, W. P., Lewis, S. A., Ruth, M. J., Muntean, G. G., Smith, R. C., and Stang, J. H., "Resolving EGR Distribution and Mixing" SAE Paper 2002, No. 2002-01-2882

[13] Shahabi, P. B., Niazmand, H., Modarres Razavi, M. R., "Particle Tracking Based Method for Evaluation of Cylinder-to-Cylinder Distribution of EGR/Blowby" under review, Particle & Particle Systems characterization

[14] Bashi Shahabi, P., "EGR/Blowby localization on intake manifold", PhD thesis in Mechanical enginnering, Ferdowsi University of Mashhad, 2011.

[15] Chen, A., Sparrow, E. M., "Turbulent Modeling of Flow in a Distribution manifold", Int. J. Heat Mass Transfer 2009, 52, 1573-1581.

[16] Kale, S. C., Ganesan, V., "Investigation of the Flow Field in the Various Regions of Intake Manifold of a S.I. Engine", Indian J. Eng. Mat. Sci. 2004, 11, 85–92.

[17] Jones, G. F., Galliera, J. M., "Isothermal Flow Distribution in Coupled Manifolds: Comparison of Results from CFD and an Integral Model", Proc. ASME Fluids Eng. Div. 1998, 247, 189–195